

A weight function-critical plane approach for low-cycle fatigue under variable amplitude multiaxial loading

X. CHEN¹, D. JIN^{2,3} and K. S. KIM³

¹School of Chemical Engineering & Technology, Tianjin University, Tianjin, 300072, P. R. China, ²School of Mechanical Engineering, Shenyang Institute of Chemical Technology, ³Department of Mechanical Engineering, Pohang University of Science and Technology, Pohang 790-784, South Korea

Received in final form 20 January 2006

ABSTRACT Low-cycle fatigue data of type 304 stainless steel obtained under axial-torsional loading of variable amplitudes are analyzed using four multiaxial fatigue parameters: SWT, KBM, FS and LKN. Rainflow cycle counting and Morrow's plastic work interaction rule are used to calculate fatigue damage. The performance of a fatigue model is dependent on the fatigue parameter, the critical plane and the damage accumulation rule employed in the model. The conservatism and non-conservatism of predicted lives are examined for some combinations of these variables. A new critical plane called the weight function-critical plane is introduced for variable amplitude loading. This approach is found to improve the KBM-based life predictions.

Keywords damage accumulation rule; irregular loading; multiaxial fatigue; rainflow cycle counting; weight function-critical plane approach.

INTRODUCTION

Engineering components are often subjected to complex multiaxial loading in which not only the amplitude of loading changes with time but also the principal axes rotate. There have been numerous researches under proportional and non-proportional multiaxial loading of constant and variable amplitudes. The works cited in the following reflect only a little fraction of the literature directly related.

Findley *et al.*¹ initially defined the critical plane as the plane subjected to the largest cycle of shear strain for high-cycle fatigue, and then the concept was applied in low-cycle fatigue. Smith *et al.*² (SWT) proposed a fatigue model for materials showing normal fracture. The maximum normal strain plane was considered as the critical plane in the model. Wang and Brown³ applied the Kandil–Brown–Miller⁴ (KBM) model to variable amplitude tension–torsion loading with the maximum shear strain range plane as the critical plane. Fatemi and Socie⁵ (FS) proposed a fatigue model for shear fracture materials. The maximum shear strain plane was considered as the critical plane and the normal stress on the plane was used to replace the normal strain of the KBM model. Socie⁶ proposed that the maximum shear or normal strain plane as the critical plane depending on the material, load-

ing mode and strain amplitude. Then Bannantine and Socie⁷ employed a method where the maximum damage plane is considered as the plane where life is evaluated. The controversy with the critical plane approach based on the maximum strain range is that while the observed crack initiation plane is the critical plane, shear or normal, the maximum value of the fatigue parameter employed for life calculation is achieved on a different plane.⁸ Recently, energy approaches have been employed for fatigue prediction under random loading. An energy model accounting for normal and shear deformation for predicting fatigue lives under variable amplitude multiaxial loading was used by Lee *et al.*⁹ (LKN) to predict the fatigue lives of carbon steel (S45C), low alloy steel (SNCM439, SNCM630) and type 304 stainless steel under tension–torsion loading. The total hysteresis energy was used by Tchankov¹⁰ as a fatigue parameter. Lagoda *et al.*^{11–13} proposed a normal strain energy criterion for uniaxial random loading in which negative energy was used for compression, and this model was also used in biaxial random tension–compression high-cycle fatigue regime. Lachowicz¹⁴ proposed a method of identification and calculation of the damage by strain energy density under cyclic random loading. The method consists of integration of the history of the instantaneous strain energy. A probabilistic method¹⁵ and a weight-function method¹⁶ were used to determine fatigue lives under random loading

Correspondence: X. Chen. E-mail: xchen@tju.edu.cn

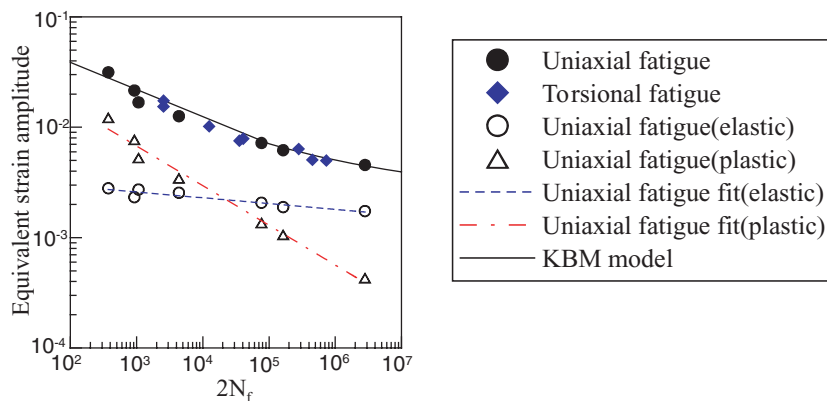


Fig. 1 KBM parameter versus fatigue life curve.

and fracture plane orientations in multiaxial high-cycle fatigue of metals. Rainflow counting algorithms were developed for uniaxial fatigue and they were later modified to use with multiaxial fatigue.^{17–20} It is a common practice that a life computation procedure employs rainflow cycle counting on an appropriate strain–stress history on the critical plane and a linear damage rule (LDR). But the deficiencies with the LDR are its load-level and load-sequence independence, and lack of load-interaction accountability. Thus, damage is often underestimated by the LDR. Morrow’s plastic work interaction rule,²¹ which will be implemented in this study, yields more conservative results than the LDR.

In this paper, three fatigue parameters are employed for correlating low-cycle fatigue data under variable amplitude multiaxial loading, i.e. SWT, KBM and FS. A life computation procedure is employed in which rainflow cycle counting on a suitable plane for the fatigue parameter and Morrow’s plastic work interaction rule are used to calculate the damage. Considering loading history-dependent nature of the critical plane under variable amplitude multiaxial loading, a new concept of the critical plane is attempted by applying a weight function on the strain range-based critical plane. The consequences will be examined.

MULTIAXIAL FATIGUE CRITERIA

The multiaxial fatigue criteria employed in this paper are given as follows:

1 The SWT model²

$$\frac{\Delta \varepsilon_n}{2} \sigma_n^{\max} = \frac{\sigma_f^{\prime 2}}{E} (2N_f)^{2b} + \sigma_f' \varepsilon_f' (2N_f)^{b+c}. \tag{1}$$

2 The KBM model⁴

In this study, a shear strain-normal strain parameter was employed, which was introduced by Kandil *et al.*⁴ and recently applied to variable amplitude loading by Wang and

Brown.^{3,17,18}

$$\frac{\Delta \gamma}{2} + s \varepsilon_n^* = [1 + \nu + (1 - \nu)s] \frac{\sigma_f' - \sigma_0}{E} (2N_f)^b + (1.5 + 0.5s) \varepsilon_f' (2N_f)^c, \tag{2}$$

where $\Delta \gamma$ is the maximum shear strain range, ε_n^* is the normal strain excursion on the plane where the maximum shear strain range occurs. s is the material constant that can be determined by uniaxial and torsional tests. For type 304 stainless steel used for evaluation in this study, $s = 1.2$. The relationship between the KBM parameter and fatigue life is given in Fig. 1.

3 The FS model⁵

$$\frac{\Delta \gamma_{\max}}{2} \left(1 + k \frac{\sigma_n^{\max}}{\sigma_y} \right) = \frac{\tau_f'}{G} (2N_f)^{b_0} + \gamma_f' (2N_f)^{c_0}, \tag{3}$$

where $\Delta \gamma_{\max}$ is the maximum shear strain range, σ_n^{\max} is the maximum normal stress on the plane of $\Delta \gamma_{\max}$, σ_y is the yield strength and k is a constant determined experimentally from axial and torsional fatigue data⁵ in a similar manner as s for the KBM parameter, and $k = 0.85$ for the current material.

In the above equations, $\sigma_f'(\tau_f'), \varepsilon_f'(\gamma_f'), b(b_0)$ and $c(c_0)$ are fatigue properties in Coffin–Manson equation from uniaxial (torsional) tests. The fatigue properties from fatigue curves are given in Table 1. E is the elastic modulus, G is the shear modulus, σ_n^0 is the mean normal stress, ε_n^* is the normal strain excursion, σ_y is the yield stress of material, $\Delta \sigma_n$ and $\Delta \tau_n$ are the normal and shear stress ranges, respectively, on the critical plane.

EXPERIMENTS

The material used in this investigation is type 304 stainless steel. The fatigue data have been previously reported.^{8,9} A brief outline of the experiment is given here for continuity. The specimen had a tubular geometry with an outer diameter of 12.5 mm and an inner diameter of 10 mm at the gage section. The material had the following properties:

Table 1 Fatigue properties of the material

Uniaxial properties	Torsional properties
Fatigue strength coefficient, σ'_f (MPa) 845	Shear fatigue strength coefficient, τ'_f (MPa) 831
Fatigue strength exponent, b -0.0518	Shear fatigue strength exponent, b_0 -0.1003
Fatigue ductility coefficient, ϵ'_f 0.23	Shear fatigue ductility coefficient, γ'_f 0.1402
Fatigue ductility exponent, c -0.416	Shear fatigue ductility exponent, c_0 -0.339

elastic modulus 171 GPa, yield stress 405 MPa, ultimate tensile strength 754 MPa, shear modulus 66 GPa, and Poisson's ratio 0.3. Fatigue tests were conducted on an MTS tension-torsion machine under strain control through a biaxial extensometer mounted on the outside of the specimen gage section. The experiments were conducted at room temperature. Failure was defined as a drop of 10% in axial loading for axial tests and axial-torsional tests from stable values, and a drop of 10% in torque for torsion tests. The loading paths are shown in Table 2. The number followed acronym of the loading path is specimen number. The numerical values of strain history in one loading block and the experimental results are given in the previous works.^{8,9}

RESULTS AND DISCUSSION

Morrow's plastic work interaction rule will be used in this study for damage accumulation.²¹ It can be written as

$$D_i = \frac{n_i}{N_i} \left(\frac{\sigma_i}{\sigma_m} \right)^d, \quad D = \sum_i D_i = \sum_i \frac{n_i}{N_i} \left(\frac{\sigma_i}{\sigma_m} \right)^d, \quad (5)$$

where σ_m is the maximum stress amplitude in the stress history considered, n_i is the number of stress peak at level σ_i , N_i is the number of cycles to failure at stress amplitude σ_i , and d is Morrow's plastic work interaction exponent. The exponent can be interpreted as the material's sensitivity to the variable-amplitude stress history. The nonlinear damage rule reduces to the LDR if the exponent d is chosen to be zero. It is interesting to note that Morrow's plastic work interaction damage rule has exactly the same form as the Corten-Dorlan cumulative damage theory²² although they were derived from different perspectives and based on different assumptions. For the current material, $d = -0.5$ is suitable.

Three fatigue models previously defined (SWT, KBM and FS) are used in conjunction with rainflow cycle counting on the shear strain history for KBM and FS model, and the normal strain history for SWT model. Morrow's plastic work interaction rule was employed for damage computation. The stress and strain are calculated for planes with angle $0^\circ \leq \theta \leq 180^\circ$ from the axis of the specimen with an increment of 1° . The critical plane is the maximum

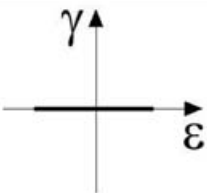
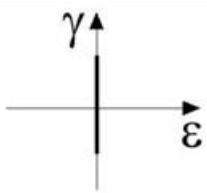
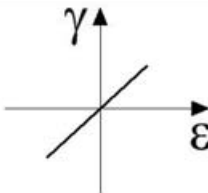
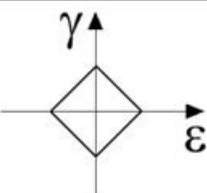
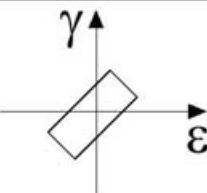
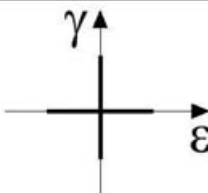
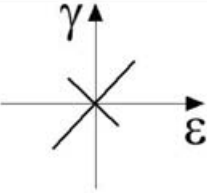
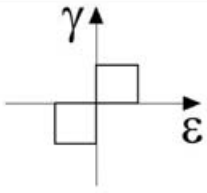
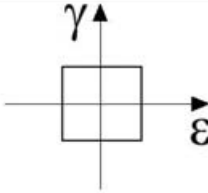
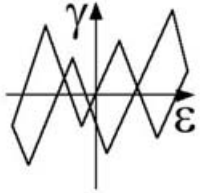
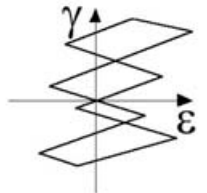
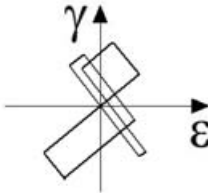
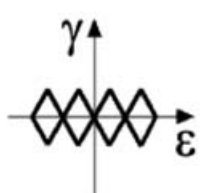
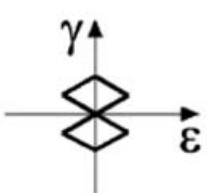
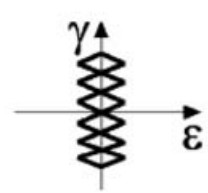
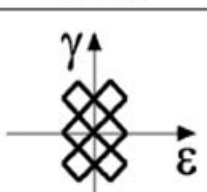
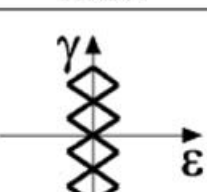
normal strain plane for the SWT parameter, and the maximum shear strain plane for the KBM and FS models.

Previous researches^{8,9} showed that this material showed a mixed cyclic hardening and softening behaviour both in axial and torsional tests. Softening occurred at smaller strain amplitudes and hardening occurred at larger strain amplitudes. At small amplitudes in torsion, the material showed slight hardening after initial softening, the overall effect being softening. Additional hardening in 90° out-of-phase loading was observed.

The prediction results of all models are shown in Figs 2–4. The solid lines in these figures represent perfect correlation and the dotted lines are for the factor-2 band. It is seen that the non-conservative prediction results are obtained by the SWT model, especially for TV, AAT and TnA loading paths. The previous research⁸ demonstrated that under axial loading the present material fails in normal mode, whereas under torsion it showed shear fracture in the low-cycle regime and normal fracture in the high-cycle regime. For TV specimens, the crack propagated in shear mode and therefore it is not surprising that the performance of this model is relatively poor. For AAT specimen, the level of input shear strain is much larger than that of axial strain. The results of analysis indicate that the non-conservatism of predicted lives is related to the influence of shear strain. The SWT model considers the effect of normal strain and stress only, and the shear strain and stress does not play a role. The KBM model gives better predictions than the SWT model though the non-conservative trend for partial TnA and AV specimens still exists. The predictions for TV specimens were improved by this model. The parameter in this model is given by the shear strain and normal strain on the maximum shear strain plane, so it will give better life prediction for the path where shear strain is much larger than axial strain. The life predictions for the FS model are better than two previous models. The normal stress is used instead of normal strain in this model, and the effect of additional hardening under irregular loading path is treated better.

In Figs 5 and 6, the maximum damage plane was considered as the critical plane and the KBM and FS models were used for fatigue life prediction. In Figs 3 and 4 the maximum shear strain range ($\Delta\gamma_{\max}$) plane was considered as critical plane, and in Figs 5 and 6 the maximum damage

Table 2 Strain paths for variable amplitude/irregular loading tests

		
AV	TV	CP, PV
		
COP	COP	AAT
		
AP	TB	B
		
R01	R02	R03
		
T2A 301	T1A201	T1A601
		
T4A 10X	T1A 40X	

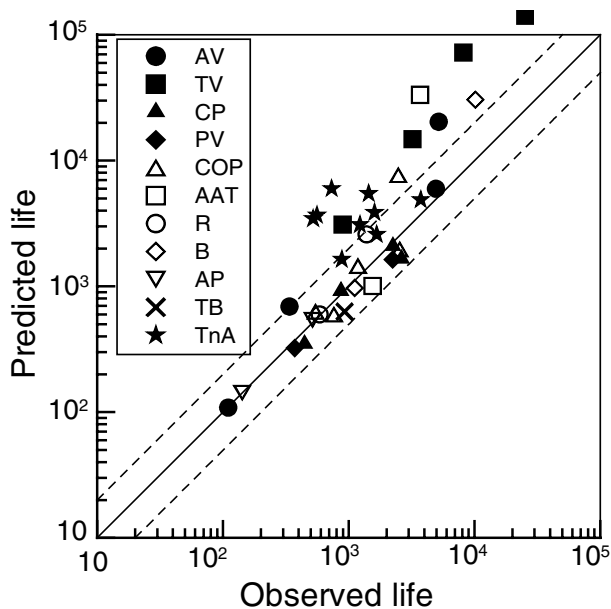


Fig. 2 Fatigue life prediction based on the SWT parameter.

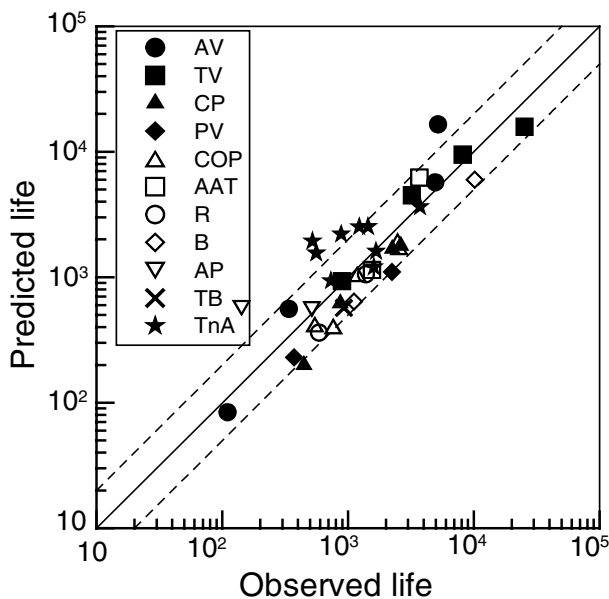


Fig. 4 Fatigue life prediction based on the FS parameter.

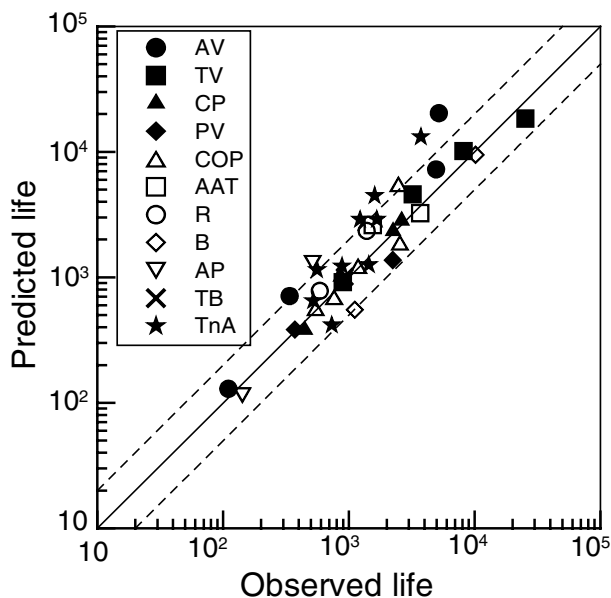


Fig. 3 Fatigue life prediction based on the KBM parameter.

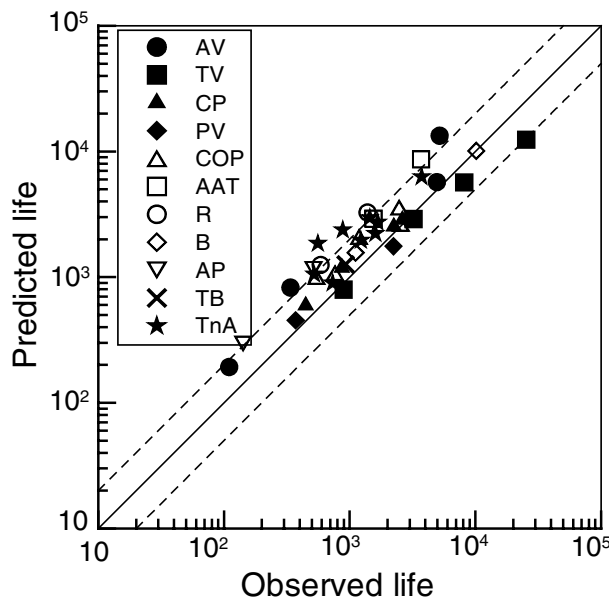


Fig. 5 Fatigue life prediction based on the KBM parameter on the maximum damage plane.

(D_{max}) plane was considered as critical plane. The plane where D_{max} is attained in analysis was different from the $\Delta\gamma_{max}$ plane in all test conditions. The damage parameters were different due to the different critical plane and the different lives were gained. On the whole, the maximum damage plane approach is more conservative than that of the maximum shear strain range plane. By comparing Fig. 5 with Fig. 3, and Fig. 6 with Fig. 4, it is found that the results of the KBM model are improved and that the

data points in the FS model are shifted to the conservative side slightly.

THE WEIGHT FUNCTION-CRITICAL PLANE APPROACH

The states of stress and strain under fatigue loading are generally time varying, and they may be complex multi-axial states. A plane may experience maximum damage at

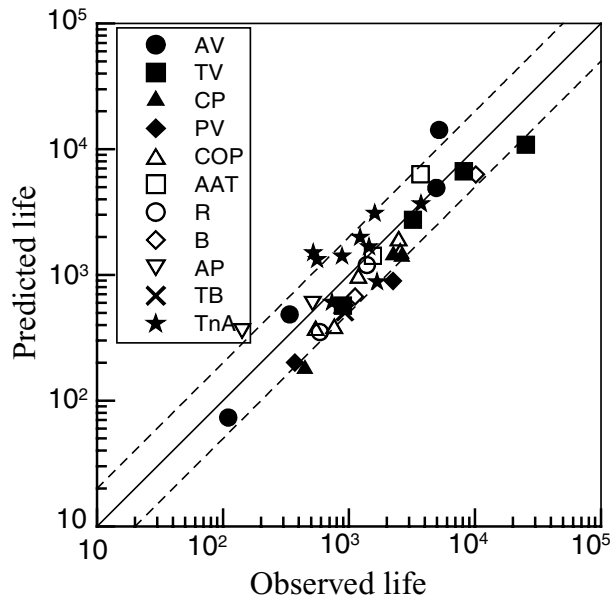


Fig. 6 Fatigue life prediction based on the FS parameter on the maximum damage plane.

some time points, but another plane may sustain greater overall damage, though diffused over time. Because of irregularity of the loading path and amplitude under random multiaxial loading, it is expedient to average the damage over a period of time. The expected maximum shear strain plane under multiaxial random loading are theoretically obtained by averaging the instantaneous values of the maximum shear strain plane through some suitable functions which are assumed to take into account the main factors influencing fatigue behaviours. The averaging could be performed, for example, by using an appropriate weight function method that takes into account the shear strain on the instantaneous maximum shear strain plane.

The stress and strain on all planes are calculated for angles $0^\circ \leq \theta \leq 180^\circ$ from the axis of the specimen with an increment of 1° . The shear strain and normal strain on arbitrary planes change with the angle θ and time. The variation is shown in Fig. 7 for the R03 path as an example. It is seen that the variation is significant and that there are several shear strain peaks. This instantaneous nature of the critical plane should be considered when the critical plane for the whole spectrum is sought. A new critical plane is defined by applying a weight function on the instantaneous critical plane.

For materials showing shear fracture, the weight function in this study is defined by

$$\bar{\theta} = \frac{1}{W} \sum_{i=1}^n \theta(t_i) w(t_i), \quad (6)$$

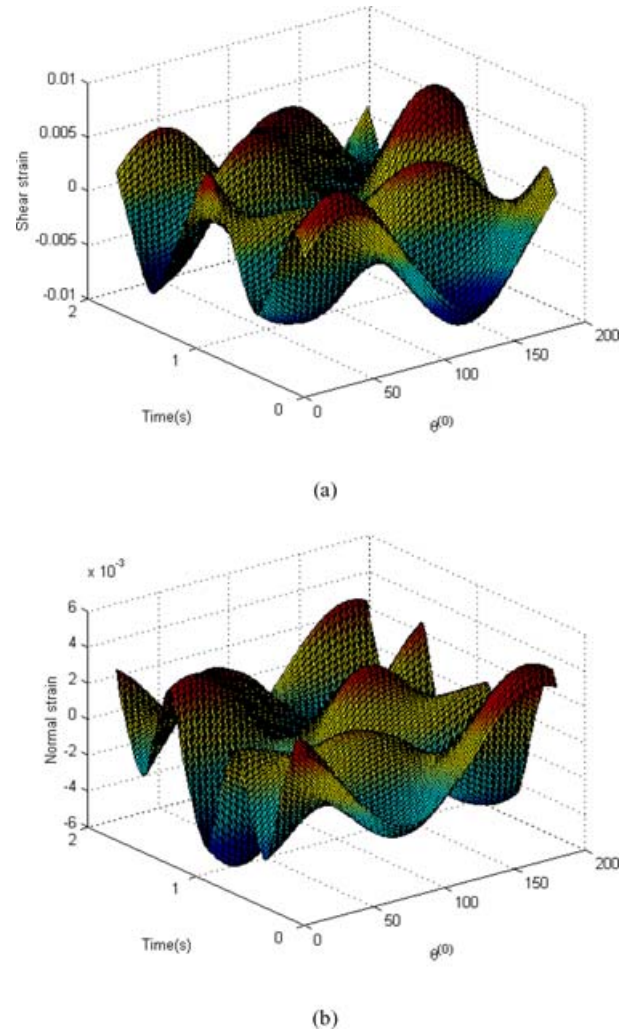


Fig. 7 Variation of shear strain and normal strain with orientation (R03 path); (a) shear strain, (b) normal strain.

where $\theta(t_i)$ is the maximum shear strain plane at an arbitrary time t_i , $w(t_i)$ is the weight for $\theta(t_i)$ and it is related to the maximum shear strain as

$$w(t_i) = \frac{\gamma_{ti} - \gamma_{\min}}{\gamma_{\max} - \gamma_{\min}}, \quad (7)$$

where γ_{\min} and γ_{\max} are the minimum and maximum shear strain in the loading block, γ_{ti} is the shear strain at time t_i , W is the sum of $w(t_i)$ over the time period of the loading block. The plane $\bar{\theta}$ is considered as the critical plane, and the fatigue damage is evaluated on this critical plane to predict life.

The difference between the maximum shear strain plane and the weight function-based critical plane depends on the loading path. The difference may be large for some loading paths but others may show no difference. Variations in weight function and the maximum shear strain

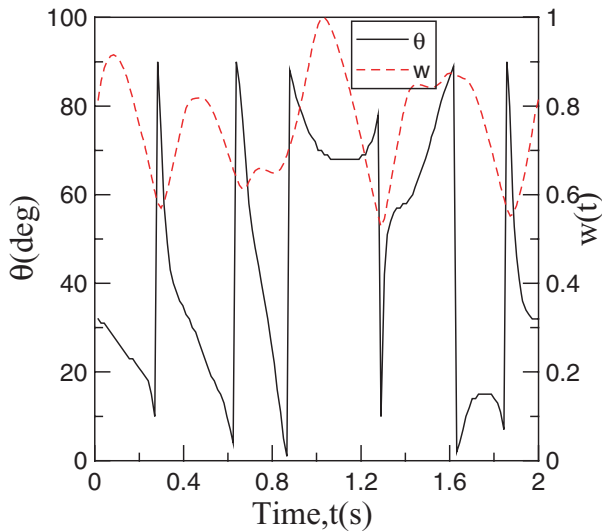


Fig. 8 Variation of the weight function and the maximum shear strain plane with time for R03 specimen.

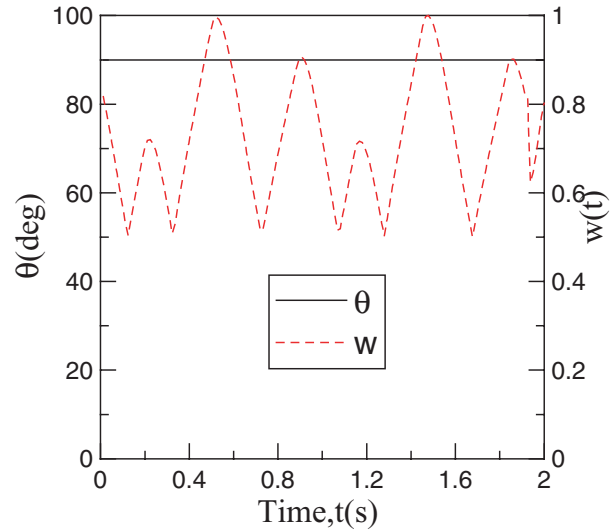


Fig. 10 Variation of the weight function and the maximum shear strain plane with time for TV02 specimen.

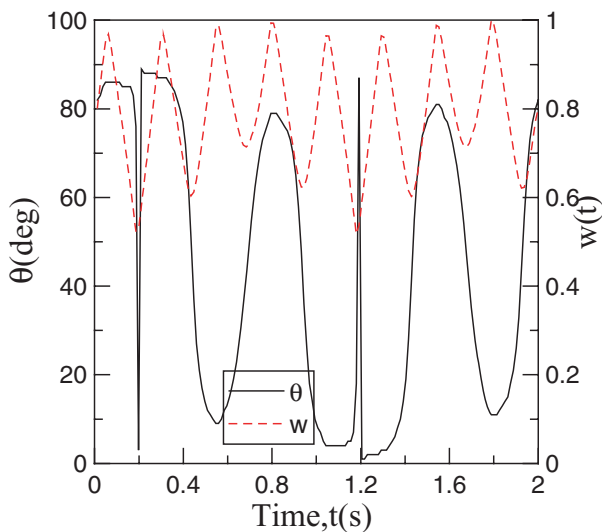


Fig. 9 Variation of the weight function and the maximum shear strain plane with time for T4a101 specimen.

plane with time for loading paths R03 and T4A101 are shown in Figs 8 and 9, respectively. It is found that for the two loading paths, the variation is fairly large. So it is necessary to consider the weight function for these loading paths. For TV02 specimen shown in Fig. 10, the weight function changes much with time but the maximum shear strain plane remains unchanged. In this case, the weight function approach is not needed. It may be said that the weight function approach is unnecessary for proportional loading paths.

The weight function-critical plane approach has been used with the KBM fatigue parameter and the results

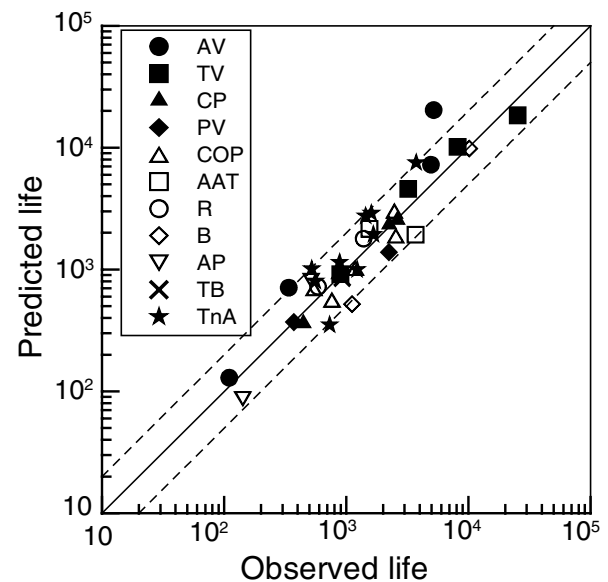


Fig. 11 Fatigue life prediction based on the weight function-critical plane method.

are shown in Fig. 11. It is found the correlations are good. The prediction results are non-conservative for the AV loading path. This approach improves the prediction results for TnA loading paths; compared with Fig. 3.

For a statistical evaluation of the damage prediction methods, the following three items – (error criterion, mean value and the coefficient of variance) were considered²³:

$E_f =$ The number of data points falling in the range $0.5 \leq N_{\text{esti}}/N_{\text{test}} \leq 2$ divided by The number of total data points,

$$E_{\text{mean}} = 1 - |1 - \text{Mean}|,$$

where Mean is the arithmetic mean of the ratio $N_{\text{esti}}/N_{\text{test}}$. N_{esti} means the prediction life by the different models and N_{test} means the test result.

$$E_{\text{CV}} = 1 - |\text{CV}|$$

where CV is the coefficient of variance given by the ratio between standard deviation and mean.

E_f is the error criterion that is most frequently used to evaluate the estimation method. The error criterion evaluates the accuracy of estimation in terms of the fraction of data falling within a scatter band of a specified factor 2. The closer the value of E_f is to 1, the better the estimation is. The mean value of data was additionally employed because the error criterion E_f cannot evaluate accurately the deviation of data value from the ideal value of $N_{\text{esti}}/N_{\text{test}} = 1$. The Mean can be used to judge whether the method is conservative (Mean < 1) or non-conservative (Mean > 1). The coefficient of variance and E_{CV} are measures of normalized scatter.

Assuming for convenience that the three statistical values are equally important, the evaluation of the performance of individual methods was carried out using the mean of E values defined above, i.e.

$$\hat{E} = (E_f + E_{\text{mean}} + E_{\text{CV}})/3 \quad (8)$$

Another factor \bar{E} , which is a measure of scatter, is given by

$$\bar{E} = \frac{1}{n} \sum_{i=1}^n |\text{Err}_i|, \quad \text{Err} = \log(N_{\text{esti}}/N_{\text{test}}) \quad (9)$$

Table 3 shows a comparison of damage calculation methods in terms of statistical values described above. The closer the value of E_{CV} and \hat{E} is to 1, the better the estimation is. The smaller the value of \bar{E} is, the better the estimation is. If \hat{E} is larger than 1, the predictions will

Table 3 Comparison of different parameters in terms of statistical values

Damage parameter	E_f (%)	E_{CV}	\bar{E} (%)	\hat{E}
SWT	59.5	0.85	32.3	1.35
KBM	75.7	0.91	17.5	1.03
FS	78.4	0.88	20.5	0.97
KBM_max	68.1	0.94	21.1	1.08
FS_max	81.1	0.89	20.9	0.92
KBM_wt	86.5	0.92	15.5	1.002

be overall non-conservative. Otherwise the predictions are conservative. The bold-faced numbers in the table are for the model with best performance for each statistical variable.

The SWT parameter based on the maximum normal strain plane gives non-conservative results. The KBM parameter based on the maximum damage plane also gives non-conservative predictions. The KBM parameter based on the weight function-critical plane gives better predictions according to E_f . For E_{CV} , the KBM parameter based on the maximum damage plane gives better results but on the whole the predictions are more non-conservative. The values of \bar{E} say that the KBM parameter based on the weight function-critical plane provides better results and that the SWT parameter gives poorer predictions.

The prediction capability of the different fatigue parameters varies depending on the statistical value being considered. Thus, it has some merit to consider the combined influence of different statistical values. The KBM parameter based on the weight function-critical plane gives better predictions in view of \hat{E} compared with other KBM-based approaches.

CONCLUSIONS

Three damage models (SWT, KBM, FS) are employed for correlating low-cycle fatigue data of type 304 stainless steel under variable amplitude multiaxial loading. A life computation procedure is employed in which rain-flow counting on an appropriate plane for each model and Morrow's plastic work interaction rule are used to calculate the damage. The prediction results show that the SWT model gives non-conservative results for torsion and torsion-dominant loading paths. The KBM model gives better results for these loading paths than the SWT model but non-conservative for part of torsion-dominant loading paths. The FS model gives better results than the KBM model. The approach where the maximum damage plane is considered as the critical plane is found non-conservative for the KBM model. The FS model gave good correlation – slightly more conservative than the maximum shear strain plane approach. The weight function – critical plane approach was tried with the KBM model and Morrow's damage rule. It improved the results based on the other critical planes for the same parameter, and the results appear to be good.

Acknowledgements

The authors gratefully acknowledge financial support for this work from National Natural Science Foundation of China (No. 10272080) and the Teaching and Research Award Program for Outstanding Young Teachers in Higher Education Institutions of MOE, P.R.C. The authors are also thankful for the partial financial support

provided from the Brain Korea 21 Program at Pohang University of Science and Technology.

REFERENCES

- 1 Findley, W. N., Coleman, J. J. and Handley, B. C. (1956) Theory for combined bending and torsion fatigue with data for 4340 steel. In: *International conference on fatigue of metals, New York, 1956*. The Institution of Mechanical Engineers, pp. 150–157.
- 2 Smith, K. N., Watson, P. and Topper, T. H. (1970) A stress-strain function for the fatigue of metals. *J. Mater.* **5**, 767–776.
- 3 Wang, C. H. and Brown, M. W. (1993) A path-independent parameter for fatigue under proportional and non-proportional loading. *Fatigue Fract. Engng Mater. Struct.* **16**, 1285–1298.
- 4 Kandil, F. A., Brown, M. W. and Miller, K. J. (1982) Biaxial low-cycle fatigue fracture of 316 stainless steel at elevated temperature. *Met. Soc. London* **280**, 203–210.
- 5 Fatemi, A. and Socie, D. F. (1988) A critical plane approach to multiaxial fatigue damage including out-of-plane loading. *Fatigue Fract. Engng Mater. Struct.* **14**, 149–165.
- 6 Socie, D. F. (1987) Multiaxial fatigue damage models. *Trans. ASME, J. Engng Mater. Technol.* **109**, 293–298.
- 7 Bannantine, J. A. and Socie, D. F. (1991) Multiaxial fatigue life estimation techniques. In: *Advances in Fatigue Lifetime Predictive Techniques, ASTM STP 1122* (Edited by M. Mitchell & R. Langraf). American Society for Testing and Materials, Philadelphia, PA, pp. 249–275.
- 8 Kim, K. S., Lee, B. L. and Park, J. C. (2000) Biaxial fatigue of stainless steel 304 under irregular loading. In: *Fatigue and Fracture Mechanics: ASTM STP 1389* (Edited by G. R. Halford & Gallagher). American Society for Testing and Materials, West Conshohocken, pp. 79–93.
- 9 Lee, B. L., Kim, K. S. and Nam, K. M. (2003) Fatigue analysis under variable amplitude loading using an energy parameter. *Int. J. Fatigue* **25**, 621–631.
- 10 Tchankov, D. S. and Vesselinov, K. V. (1998) Fatigue life prediction under random loading using total hysteresis energy. *Int. J. Press. Vessels. Pip.* **75**, 955–960.
- 11 Lagoda, T., Macha, E. and Bedkowski, W. (1999) A critical plane approach based on energy concepts: application to biaxial random tension compression high-cycle fatigue regime. *Int. J. Fatigue* **21**, 431–443.
- 12 Lagoda, T. (2001) Energy models for fatigue life estimation under uniaxial random loading, Part I: The model elaboration. *Int. J. Fatigue* **23**, 467–480.
- 13 Lagoda, T. (2001) Energy models for fatigue life estimation under uniaxial random loading, Part II: verification of the model. *Int. J. Fatigue* **23**, 481–489.
- 14 Lachowicz, C. T. (2001) Calculation of the elastic-plastic strain energy density under cyclic and random loading. *Int. J. Fatigue* **23**, 643–652.
- 15 Lee, B. H. and Lee, S. B. (2000) Stochastic modeling of low-cycle fatigue damage in 316L stainless steel under variable multiaxial loading. *Fatigue Fract. Engng Mater. Struct.* **23**, 1007–1018.
- 16 Carpinteri, A., Macha, E., Brighenti, R. and Spagnoli, A. (1999) Expected principal stress directions under multiaxial random loading. Part I: theoretical aspects of the weight function method. *Int. J. Fatigue* **21**, 83–88.
- 17 Wang, C. H. and Brown, M. W. (1996) Life prediction techniques for variable amplitude multiaxial fatigue-Part 1: theories. *ASME Trans. J. Engng Mater. Technol.* **18**, 367–370.
- 18 Wang, C. H. and Brown, M. W. (1996) Life prediction techniques for variable amplitude multiaxial fatigue-Part 2: comparison with experimental results. *ASME Trans. J. Engng Mater. Technol.* **18**, 371–374.
- 19 Anthes, R. J. (1997) Modified rainflow counting keeping the load Sequence. *Int. J. Fatigue* **19**, 529–535.
- 20 Langlais, T. E., Vogel, J. H. and Chase, T. R. (2003) Multiaxial cycle counting for critical plane methods. *Int. J. Fatigue* **25**, 641–647.
- 21 Kurath, P., Schitoglu, H., Morrow, J. D., Deves, T. J. (1983) The effect of selected subcycle sequences in fatigue loading histories. In: *Random Fatigue Life Predictions*, ASME Publication PVP, Portland, pp. 43–60.
- 22 Corten, H. T. and Dolon, T. J. (1956) Cumulative fatigue damage. In: *Proceedings of the International Conference on Fatigue of Metals*. Institution of Mechanical Engineers, pp. 235–246.
- 23 Lee, K.-S. and Song, J.-H. (2006) Estimation methods for fatigue properties from hardness. *Int. J. Fatigue* **28**, 386–400.